Journal of Virological Methods 151 (2008) 172–180

Contents lists available at ScienceDirect

Journal of Virological Methods

journal homepage: www.elsevier.com/locate/jviromet

Recombinant hepatitis B virus core particles: Association, dissociation and encapsidation of green fluorescent protein

Khai Wooi Lee [a], Wen Siang Tan [a,b,*]

[a] Department of Microbiology, Faculty of Biotechnology and Biomolecular Sciences, Universiti Putra Malaysia, 43400 UPM Serdang, Selangor, Malaysia
[b] Institute of Biosciences, Universiti Putra Malaysia, 43400 UPM Serdang, Selangor, Malaysia

ARTICLE INFO

Article history:
Received 26 February 2008
Received in revised form 9 May 2008
Accepted 14 May 2008
Available online 27 June 2008

Keywords:
Hepatitis B virus capsid
Denaturing agent
Capsid assembly
Hepatitis B core antigen
Green fluorescent protein
Protein encapsidation

ABSTRACT

The recombinant hepatitis B virus (HBV) core antigen (HBcAg) expressed in *Escherichia coli* self-assembles into icosahedral capsids of about 35 nm which can be exploited as gene or drug delivery vehicles. The association and dissociation properties of the C-terminally truncated HBcAg with urea and guanidine hydrochloride (GdnHCl) were studied. Transmission electron microscopy (TEM) revealed that the dissociated HBcAg was able to re-associate into particles when the applied denaturing agents were physically removed. In order to evaluate the potential of the particles in capturing molecules, purified green fluorescent protein (GFP) was applied to the dissociated HBcAg for encapsidation. The HBcAg particles harbouring the GFP molecules were purified using sucrose density gradient ultracentrifugation and analysed using native agarose gel electrophoresis and TEM. A method for the encapsidation of GFP in HBcAg particles which has the potential to capture drugs or nucleic acids was established.

1. Introduction

Hepatitis B virus (HBV) is a member of the *Hepadnaviridae* family which causes acute and chronic liver diseases, such as cirrhosis and hepatocellular carcinoma. HBV poses a major health problem worldwide which results in over a million deaths each year (Jung and Pape, 2002). The hepatitis B virion, is spherical with a diameter of about 42 nm (Dane et al., 1970). The virion is enveloped by a lipid bilayer which is derived from the endoplasmic reticulum of its host cells (Ganem, 1991). The lipid is associated with three forms of related surface antigens (HBsAg) known as long (L-), medium (M-) and short (S-) polypeptides. The L-HBsAg has been shown to interact with the viral capsid during maturation (Löffler-Mary et al., 2000; Seitz et al., 2007; Tan et al., 1999). The capsid contains only one polypeptide species of 183 residues which is also known as the core antigen (HBcAg).

HBcAg can be expressed readily in *Escherichia coli* (Burrell et al., 1979) where it assembles into small and large icosahedral particles with triangulation number of $T = 3$ and $T = 4$, respectively (Crowther et al., 1994). The large particle comprises 240 subunits with a diameter of 36 nm, while the small particle contains 180 subunits with a diameter of about 32 nm (Crowther et al., 1994). The C-terminal end of the HBcAg of about 40 residues is very rich in positively charged amino acids (Tan et al., 2003; Wingfield et al., 1995) which interact with the viral genome, a 3.2-kb partially double stranded DNA molecule (Roseman et al., 2005). Residues 141–183 are dispensable for capsid assembly (Wingfield et al., 1995), thus a truncated HBcAg mutant lacking these residues is postulated to be sufficient to depict the capsid self-assembly property (Nassal et al., 1992; Wynne et al., 1999). A truncated HBcAg containing 149 N-terminal residues is able to self-assemble into large and small icosahedral particles morphologically equivalent to those formed by the full length HBcAg (Böttcher et al., 1998; Tan et al., 2003, 2007). This mutant lacks Cys-183, the last residue of HBcAg, which is always involved in a disulfide bond formation with the Cys-183 of a different monomer (Zheng et al., 1992). In the absence of this residue, the association and dissociation of HBcAg particles can be studied in vitro.

The assembly of HBcAg particles is a very complicated process, consisting of several decisive steps. During the assembly, two α-helical hairpin-like monomers associate to form a four-helix bundle dimer. In this step, the amphipathic helical hairpin and the hydrophobic faces associate to form a dimer (Bringas, 1997; Wynne et al., 1999). The disulfide bridge between the Cys-61 of two monomers ties them together and makes the dimer a stable structural unit (Nassal et al., 1992; Zheng et al., 1992). This four-

* Corresponding author at: Department of Microbiology, Faculty of Biotechnology and Biomolecular Sciences, Universiti Putra Malaysia, 43400 UPM Serdang, Selangor, Malaysia. Tel.: +60 3 8946 6715; fax: +60 3 8943 0913.
E-mail addresses: wstan@biotech.upm.edu.my, wensiangtan@yahoo.com (W.S. Tan).

0166-0934/$ – see front matter © 2008 Elsevier B.V. All rights reserved.
doi:10.1016/j.jviromet.2008.05.025

helix bundle forms the characteristic spikes on the surface of the HBcAg particles.

The truncated version of HBcAg synthesized in *E. coli* is able to self-assemble into a stable icosahedral particle with an empty inner cavity of about 26 nm in diameter (Tan et al., 2007; Wynne et al., 1999), providing a room to package up to 240 subunits of *Staphylococcus aureus* nuclease via fusion to the C-terminal end of HBcAg (Beterams et al., 2000). The high volume cavity of the HBcAg particle (~8600 nm^3) (Beterams et al., 2000) makes it a potential nano-container for packing molecules freely in its interior room.

The use of green fluorescent protein (GFP) is described as an indicator protein to study the ability of HBcAg particles in capturing molecules in vitro. A method for capturing molecules by HBcAg particles was established. This lays the foundation for exploring the potential use of HBcAg particles as a vehicle for delivering therapeutic molecules into mammalian cells.

2. Materials and methods

2.1. Expression and purification of HBcAg and GFP

Truncated HBcAg (amino acids 3–148) was produced in *E. coli* strain W3110IQ harbouring pR1-11E plasmid as described in Tan et al. (2003). Purification of the truncated HBcAg using sucrose density gradient ultracentrifugation was as described in Tan et al. (2003). *E. coli* strain BL21 (DE3) carrying the pRSETGFP plasmid encoding the GFP from jellyfish *Aequorea victoria* (a gift by Dr. Tan Chon Seng, MARDI, Malaysia) was grown in Luria Bertani (LB) broth. The expression of the recombinant GFP containing a His-tag at its N-terminus was induced by 0.5 mM isopropyl-β-D-thiogalactopyranoside (IPTG). The recombinant protein was purified using nickel-nitrilotriacetic acid (Ni-NTA) resin as recommended by the manufacturer (HisTrap HP, Amersham Biosciences, USA). The purity of the truncated HBcAg and GFP was analysed with SDS-PAGE and it was found to be more than 90% pure. The protein concentration was determined by the Bradford assay (Bradford, 1976).

2.2. Dynamic light scattering (DLS) analysis

In order to determine the dissociation and association profiles of the HBcAg particles, the hydrodynamic radius of the particles was analysed with a dynamic light scattering instrument (DynaPro-801^{TM}, Protein Solutions Ltd., High Wycombe, UK) throughout the dissociation studies. HBcAg particles (0.25 mg/ml, 50 μL) were injected into a sample cell. The samples were illuminated by a miniature solid state laser of 25 mW power and 780 nm wavelength. Light scattered at 90° to the incident beam was detected and analysed with an autocorrelation function to deduce the translational diffusion coefficient (DT) of the molecules in the sample cell. The hydrodynamic radius (R_h) of the molecules was calculated from the DT through the Stokes–Einstein equation: $R_h = kbT/6\pi\eta DT$, where kb is Boltzman's constant, T is the absolute temperature in Kelvin, and η is the solvent viscosity.

2.3. Dissociation of HBcAg particles

The dissociation of HBcAg particles was achieved by adding aliquots of denaturant stock solutions of either 8.0 M guanidine hydrochloride (GdnHCl) or 8.0 M urea, diluted with filtered distilled water to give the desired concentrations of protein (0.25 mg/ml) and denaturants (0.0, 0.5, 1.0, 1.5, 2.0, 2.5, 3.0, 4.0 and 5.0 M). All the samples were incubated at 25 °C for 3 h. The dissociation profile of the HBcAg particles was then obtained by DLS analysis of the particle size at 25 °C. A total of 20 measurements were obtained for each sample. The dissociation profiles of the HBcAg particles were then further improved by selecting a suitable denaturant concentration against a prolonged incubation time. This step was to confirm further the dissociation time needed for 0.25 mg/ml of HBcAg particles. The profiles were achieved by treating 0.25 mg/ml HBcAg particles with the desired GdnHCl and urea concentrations which were able to dissociate the HBcAg particles. The R_h of the particles was measured immediately by DLS every 15 min for 4.5 h at 25 °C.

2.4. Association of HBcAg particles

The HBcAg particles were first dissociated by incubating them with different concentrations of GdnHCl and urea at 25 °C as described above. Before the association steps, the dissociation of the HBcAg particles was confirmed by DLS analysis. The association of the dissociated HBcAg particles was obtained by diluting the denaturant content in the samples with dialysis buffer (50 mM Tris–Cl, pH 8.0, 100 mM NaCl) to approximately 0.2 M and dialysed against the same buffer (1 L, two times) overnight at 4 °C for the elimination of denaturants from the samples. The dialysed protein was adjusted to a concentration of approximately 0.25 mg/ml by concentrating with VIVASPIN 6, 30 kDa cut-off polyethersulfone membrane (VIVASCIENCE, Germany) at 4500 × g, 4 °C, and observed under a transmission electron microscope (TEM). In the preparation for TEM analysis, protein samples (15 μL) were absorbed onto carbon-coated grids (200 mesh) and negatively stained with 2% (v/v) uranyl acetate for 5 min. The grids were

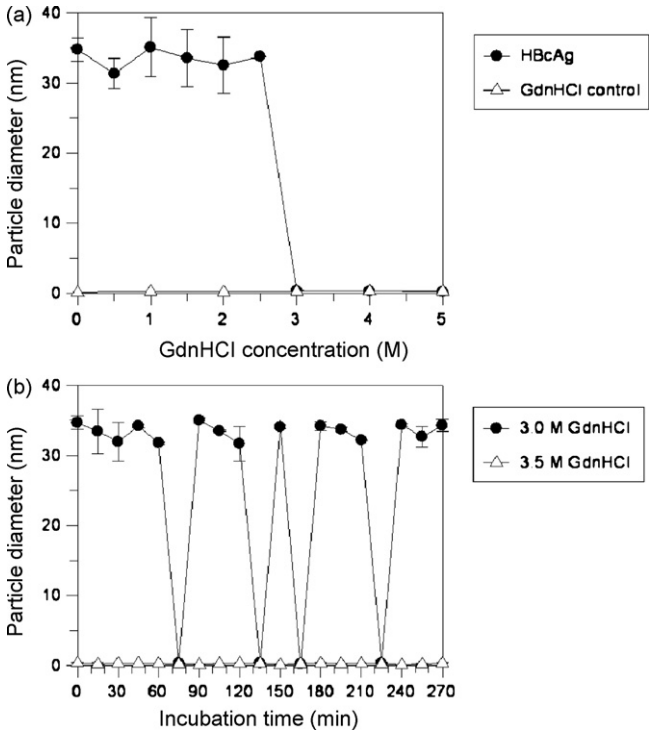

Fig. 1. Dissociation of HBcAg particles by GdnHCl. (a) Dissociation profiles of HBcAg particles (0.25 mg/ml) treated with GdnHCl from 0.0 to 5.0 M at 25 °C. The HBcAg particles were dissociated from a particle size of 33.5 ± 1.4 nm to 0.3 ± 0.1 nm at 3.0, 4.0 and 5.0 M GdnHCl. (b) Dissociation profiles of HBcAg particles (0.25 mg/ml) treated with 3.0 and 3.5 M GdnHCl at 25 °C. The HBcAg particles were first dissociated into particle size of 0.42 ± 0.0 nm at an incubation time of 75 min and fluctuated between particle size of 33.6 ± 1.0 nm and 0.4 ± 0.1 nm in the remainder of the incubation in 3.0 M GdnHCl. Treatment with 3.5 M GdnHCl dissociated the HBcAg particles instantly into a size of 0.3 ± 0.1 nm. Data points are mean ± standard deviations of triplicate determinations.

observed under a TEM (Philips HMG 400) and micrographs were taken at appropriate magnifications.

2.5. Stability of HBcAg particles at different temperatures

HBcAg samples (0.25 mg/ml) were prepared and incubated at 60, 70, 80 and 90 °C. Heat-treated samples were absorbed onto carbon-coated grids, negatively stained and analysed with a TEM as described above.

2.6. Encapsidation of green fluorescent protein by HBcAg particles

Encapsidation of GFP by HBcAg particles was performed by incubating 0.25 mg/ml HBcAg particles with 2.5 M urea at 25 °C for 3 h. The dissociation of the HBcAg particles was confirmed by DLS analysis. After the dissociation, the purified GFP (0.20 mg/ml) was added to the sample to a final volume of 20 ml. The sample was then dialysed overnight in dialysis buffer at 4 °C. The dialysed sample was concentrated with 30 kDa cut-off polyethersulfone membrane (VIVASPIN 6), applied to a sucrose gradient (8–40%, w/v) and centrifuged at 210,000 × *g*, 4 °C for 5 h as described by Tan et al. (2003). The fractions collected (500 μL) were then analysed with the Bradford assay (Bradford, 1976), SDS-PAGE and native agarose gel electrophoresis as described below. In this experiment, HBcAg particles (0.25 mg/ml, 20 ml) and GFP (0.20 mg/ml, 20 ml) treated with 2.5 M urea were used as controls.

For the purification of HBcAg subunits with diameter about 6 nm, the HBcAg particles were dissociated by mixing with 2.5 M urea and the dissociation was confirmed by DLS analysis. The subunits were concentrated with 10 kDa cut-off polyethersulfone membrane (VIVASPIN 6) and subjected to a sucrose gradient (8–40%, w/v) containing 2.5 M urea. Ultracentrifugation was performed as described above. For the encapsidation of GFP by the purified HBcAg subunits, sucrose fractions containing the subunits were mixed with the purified GFP, dialysed and fractionated on a sucrose gradient as described above.

2.7. Native agarose gel electrophoresis

In order to study the migration profiles of the HBcAg particles encapsidating GFP in a 8–40% sucrose gradient, the fractions collected were analysed on a native 1.5% (w/v) agarose gel and electrophoresed in TBE buffer (90 mM Tris–borate, 2 mM EDTA, pH 8.3) at 80 V for 2.5 h. Fluorescence was visualised by ultraviolet (UV) illu-

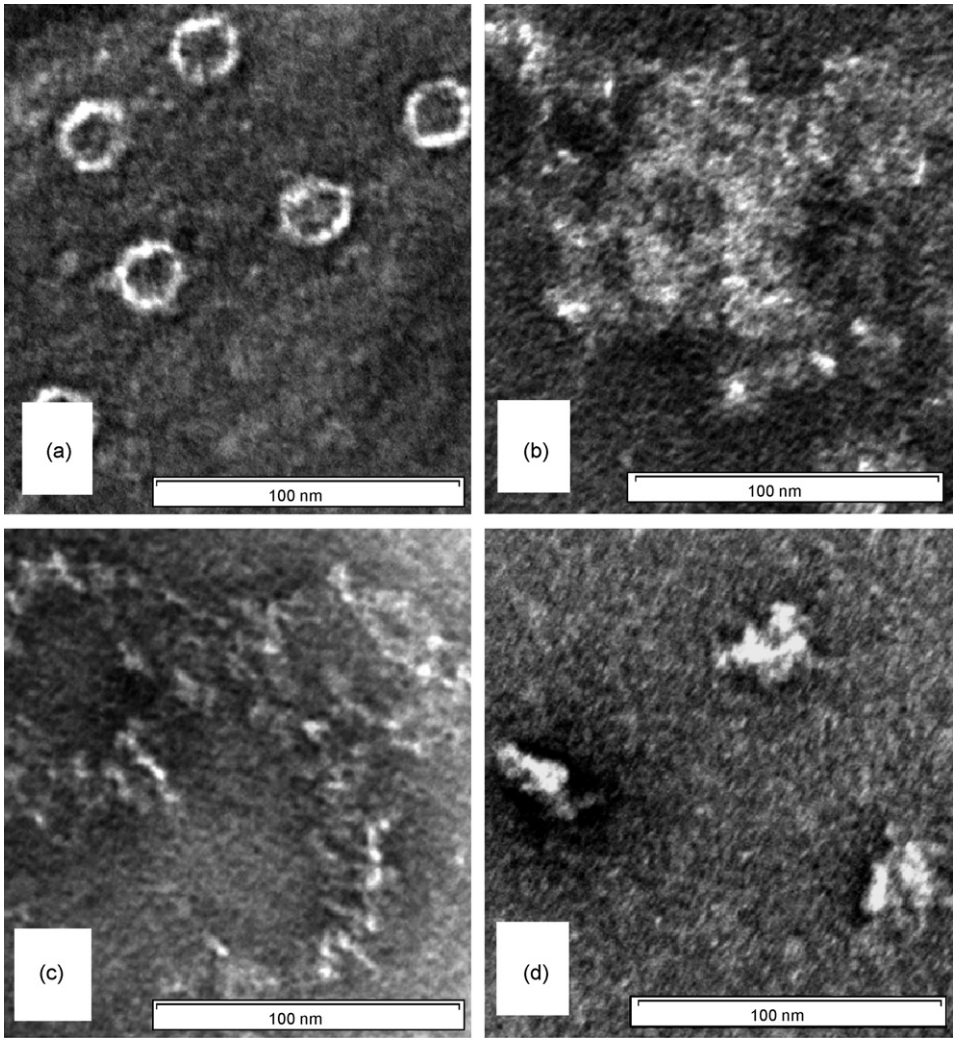

Fig. 2. Electron micrographs of HBcAg association after GdnHCl treatment. Electron micrographs showing the association profiles of HBcAg particles before and after the removal of GdnHCl at a specific incubation period at 25 °C based on the results from Fig. 1b. (a)–(c) HBcAg particles (0.25 mg/ml) were treated with 3.0 M GdnHCl, and this chemical was removed at (a) 30 min, (b) 90 min and (c) 240 min of incubation. (d) Irregular particulate structures in the presence of 3.0 M GdnHCl at 195 min of incubation. Scale bar 100 nm.

mination (312 nm) and protein bands were detected by Coomassie blue staining.

3. Results

3.1. The effect of GdnHCl on HBcAg particles

In order to study the effects of GdnHCl on the dissociation of HBcAg particles, the purified particles were incubated in 0.0–5.0 M of GdnHCl at 25 °C for 3 h. Fig. 1a shows that HBcAg particles were dissociated from a particle diameter of 33.5 ± 1.4 nm to 0.3 ± 0.1 nm in 3.0, 4.0 and 5.0 M of GdnHCl. A time course experiment revealed that HBcAg particles of about 35 nm in diameter dissociated to less than 1 nm at 75 min of incubation with 3.0 M GdnHCl. The size of the particles fluctuated between 35 and 0.5 nm from this time point onwards (Fig. 1b). To study the re-assembly of HBcAg particles, samples from various time points (30, 90 and 240 min; Fig. 1b) were dialysed, concentrated with a centrifugal filter and observed under a TEM. The typical icosahedral structure of HBcAg particles was observed in the 30-min sample (Fig. 2a) but not observed in the other two samples (Fig. 2b and c). This suggests that the 1-nm molecules formed after 75 min of incubation are likely to be the denatured HBcAg subunits which had lost their self-assembly properties. In the presence of 3.0 M GdnHCl, these denatured subunits associated into irregular particulate structures of about 35 nm (Fig. 2d). At a higher concentration of GdnHCl (3.5 M), the HBcAg particles were dissociated immediately into molecules less than 1 nm (Fig. 1b). When the GdnHCl was removed by dialysis, the denatured HBcAg did not self-assemble into particles as observed under a TEM (data not shown).

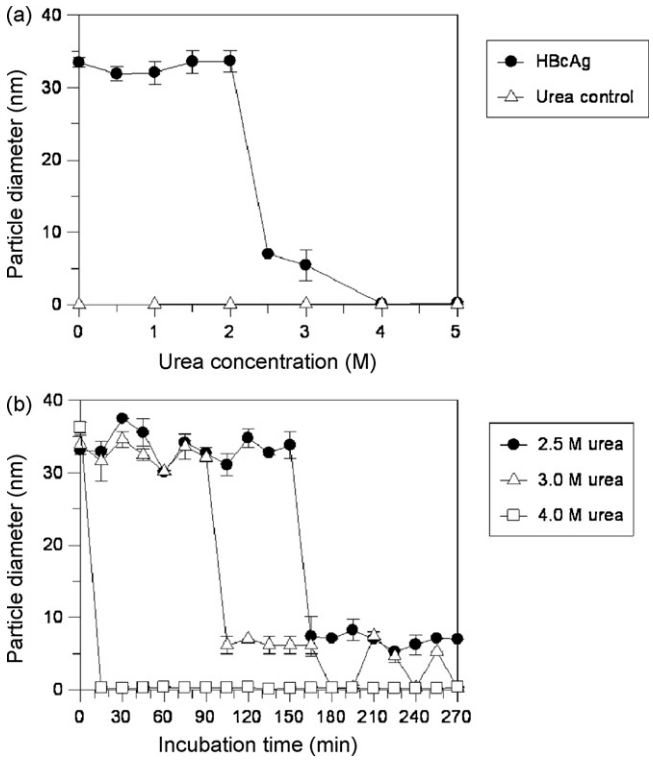

Fig. 3. Dissociation of HBcAg particles by urea. (a) Dissociation profiles of HBcAg particles (0.25 mg/ml) treated with urea from 0.0 to 5.0 M at 25 °C. The HBcAg particles were dissociated from a particle size of 32.9 ± 0.9 nm to 6.3 ± 1.0 nm at 2.5 and 3.0 M urea, and further dissociated to 0.2 ± 0.1 nm in 4.0 and 5.0 M urea. (b) Dissociation profiles of HBcAg particles (0.25 mg/ml) treated with 2.5, 3.0 and 4.0 M urea at 25 °C. The HBcAg particles were dissociated from a particle size of 33.5 ± 2.0 nm to 6.9 ± 0.9 nm after 165 min of incubation in 2.5 M urea. For the 3.0-M urea treatment, the HBcAg particles were dissociated into a particle size of 6.3 ± 0.4 nm from 32.6 ± 1.5 after the first 105 min of incubation, followed by a fluctuation of particle size between 0.3 ± 0.1 and 5.8 ± 1.5 nm in the remaining incubation time. Treatment with 4.0 M urea showed a dramatic drop in particle size at the first 15 min of incubation from 36.3 ± 0.7 to 0.3 ± 0.1 nm. Data points are mean ± standard deviations of triplicate determinations.

3.2. Dissociation and association of HBcAg particles in urea

The study of the effects of urea on HBcAg revealed that 2.5 and 3.0 M urea were able to dissociate the HBcAg particles (32.9 ± 0.9 nm) to a diameter of 6.3 ± 1.0 nm after 3 h of incubation at 25 °C (Fig. 3a). The diameter of the sample fell to below 1 nm when the concentration of urea increased to 4.0 and 5.0 M. Fig. 3b shows that the HBcAg particles dissociated from a diameter of 33.5 ± 2.0 nm to 6.9 ± 0.9 nm after 165 min of incubation in 2.5 M urea. The time needed to dissociate the particles (~35 nm) to about 6 nm is shorter (105 min) when the urea concentration was increased to 3.0 M. The TEM analysis revealed that the molecules of about 6 nm were able to self-assemble into particles of about 30 nm when the urea was removed (Fig. 4a–c). However, when the incubation time in 3.0 M urea was further extended from 165 to 270 min, the size of the molecules fluctuated between 0.3 ± 0.1 and 5.8 ± 1.5 nm (Fig. 3b). This could be the intermediate stage of the irreversible denaturation of HBcAg. Re-association of HBcAg was not detected at this stage when the urea was removed (Fig. 4d). HBcAg particles mixed with 4.0 M urea showed a dramatic drop in size from 36.3 ± 0.7 to 0.3 ± 0.1 nm in the first 15 min of incubation. A similar profile was observed for the HBcAg particles in 3.5 M of GdnHCl (Fig. 1b). At this stage, molecules with diameters less than 1 nm were not able to re-associate into HBcAg particles when the urea was removed (Fig. 4e and f).

3.3. Heat treatment on HBcAg particles

TEM analysis of the heat-treated HBcAg particles revealed that the particles remained intact with diameters of about 31 ± 4 nm at 60 and 70 °C for 1 h (data not shown). The HBcAg particles were partially ruptured at 80 °C. When the temperature was increased to 90 °C, intact HBcAg particles were not observed (data not shown). This study demonstrates that the recombinant HBcAg particles are heat stable and can withstand a temperature of 70 °C for at least 1 h.

3.4. Encapsidation of GFP by HBcAg particles

A method for the encapsidation of GFP by HBcAg particles was established. The purified HBcAg particles were first dissociated by incubating in 2.5 M urea for 3 h at 25 °C. DLS analysis confirmed that the particles were fully dissociated. Then, GFP was applied into the solution and urea was removed by dialysis. HBcAg particles harbouring the GFP were separated by sucrose density gradient ultracentrifugation. The migration of the HBcAg particles in the gradient is shown in Fig. 5. In the absence of GFP, the particles migrated in the gradient to form a peak between fractions 5–12. The second peak towards the top of the gradient (fractions 19–24) contained unassembled HBcAg and other host proteins. The migration profile was in good agreement with that demonstrated by Tan et al. (2003). Interestingly, in the presence of GFP, the first peak shifted towards the left to a higher density (fractions 4–11), indicating the presence of denser particles. In the absence of HBcAg, the GFP molecules did not enter the sucrose gradient and accumulated at the top of it (fractions 18–24).

The sucrose gradient fractions were also analysed with SDS-PAGE to confirm the migration of HBcAg and GFP in the gradient.

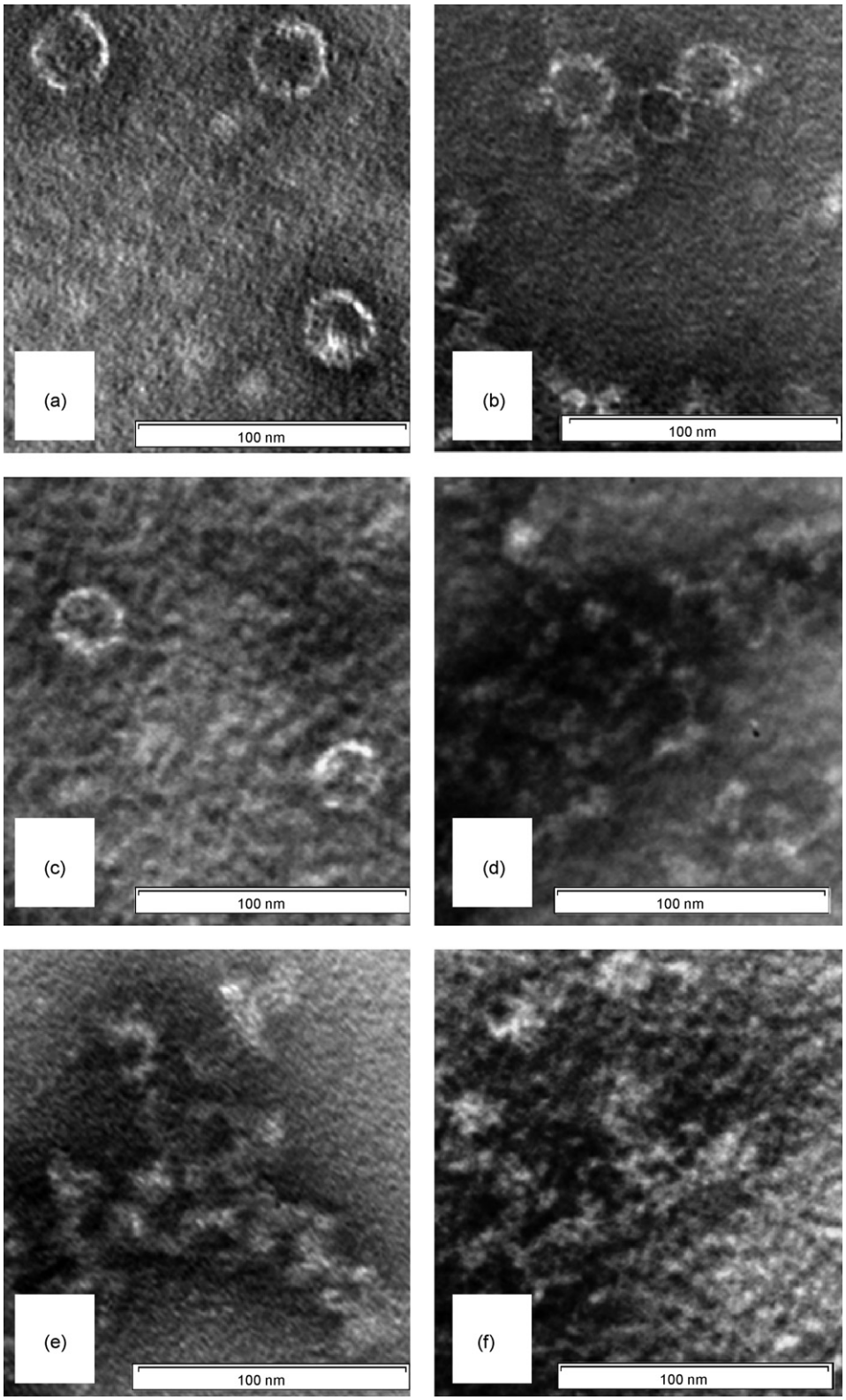

Fig. 4. Electron micrographs of HBcAg association after urea treatment. Electron micrographs showing the association profiles of HBcAg particles after the removal of urea at a specific incubation period at 25 °C based on the results from Fig. 3b. (a) and (b) HBcAg particles (0.25 mg/ml) were treated with 2.5 M urea, and this chemical was removed at (a) 180 min of incubation and at (b) 240 min of incubation. (c) and (d) HBcAg particles (0.25 mg/ml) were treated with 3.0 M urea, and this chemical was removed at (c) 120 min of incubation and at (d) 240 min of incubation. (e) and (f) HBcAg particles (0.25 mg/ml) were treated with 4.0 M urea, and this chemical was removed at (e) 30 min of incubation and at (f) 240 min of incubation. Scale bar 100 nm.

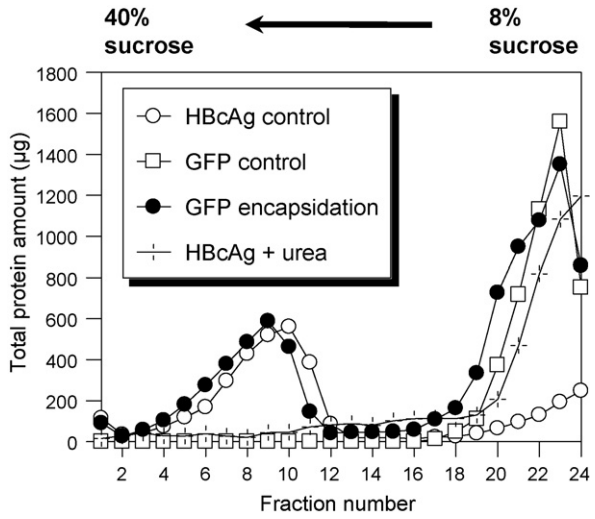

Fig. 5. Sucrose density gradient ultracentrifugation. HBcAg particles harbouring GFP were separated by centrifugation on a sucrose gradient (8–40%). The total protein in each fraction (500 μL) was determined by the Bradford Assay. The HBcAg particles containing GFP (fractions 4–11) had a faster migration rate, compared to the empty HBcAg particles (fractions 5–12). The majority of the GFP and unassembled HBcAg were located at the top of the sucrose gradient (fractions 18–24). The HBcAg subunits (6 nm species) fractionated on a sucrose gradient (8–40%) containing 2.5 M urea were located at the top of the gradient (fractions 20–24).

Coomassie blue staining of the denaturing gel showed that in the absence of GFP, more HBcAg was detected between fractions 5–12 (Fig. 6a), which corresponded well with the first peak in the Bradford assay. In the presence of GFP, the HBcAg particles migrated slightly faster and more HBcAg was detected between fractions 4–11 (Fig. 6b). In addition, two faint bands of approximately 31 and 34 kDa, showed the co-migration of GFP with HBcAg in fractions 5–10 (Fig. 6b). These bands were indeed GFP as they were detected by anti-GFP monoclonal antibody in Western blot analysis (data not shown). A majority of the excess GFP molecules were located towards the top of the gradient (fractions 18–24). For the negative control containing only GFP, the protein bands of about 31 and 34 kDa accumulated in fractions 18–24 (Fig. 6c).

In order to prove that the HBcAg re-associated into particles, the fractions that made up the first peak (in the presence of GFP) were pooled, concentrated and observed under a TEM. Fig. 7 shows that the HBcAg re-assembled into icosahedral structures which were morphologically akin with the original HBcAg particles. The sucrose gradient fractions were also analysed with native agarose gels to confirm the encapsidation of GFP by HBcAg particles. Fig. 8a shows that GFP migrated together with the HBcAg particles and two green fluorescent bands were observed in fractions 5–10. The migration rate of these bands were similar to those of HBcAg particles as detected in the same gel subsequently stained with Coomassie blue (Fig. 8b), demonstrating that the GFP molecules captured in the HBcAg particles were active. The large and small HBcAg particles were well separated into two distinct bands as observed in both the UV-illuminated and the Coomassie blue-stained gels (fractions 5–10). This observation was in good agreement with that reported by Newman et al. (2003). The HBcAg particles harbouring the GFP molecules were kept for 1 month at 4 °C and native agarose gel electrophoresis showed that their migration profile was similar with the freshly prepared samples (data not shown). This

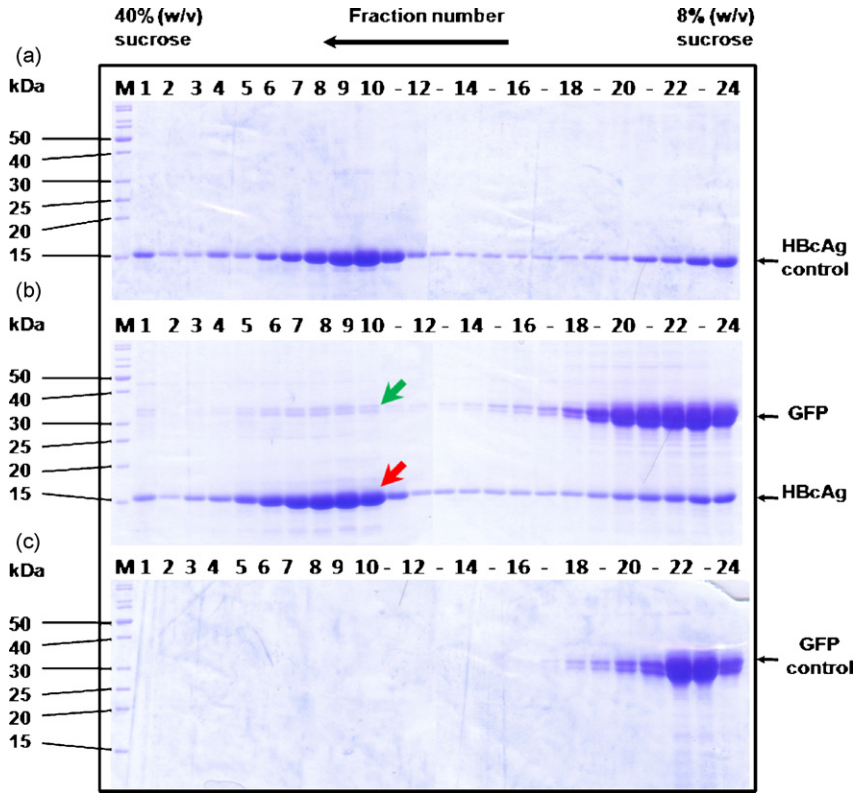

Fig. 6. Encapsidation of GFP by HBcAg particles. The GFP was encapsidated in the HBcAg particles, concentrated and subjected to 8–40% (w/v) sucrose density gradient centrifugation. Fractions (500 μL) were collected and analysed with SDS-PAGE. (a) and (c) are the HBcAg and GFP controls, respectively. (b) GFP encapsidated by HBcAg particles. The Coomassie blue-stained gel shows a conspicuous band of 17 kDa HBcAg in fractions 4–11. Two bands of approximately 31 and 34 kDa, show the co-migration of the released GFP (green arrow) with HBcAg (red arrow) in fractions 5–10. Excess GFP applied to the encapsidation process was observed at the top of the sucrose gradient. The apparent molecular masses of the protein markers (lane M) are indicated on the left. (For interpretation of the references to colour in this figure legend, the reader is referred to the web version of the article.)

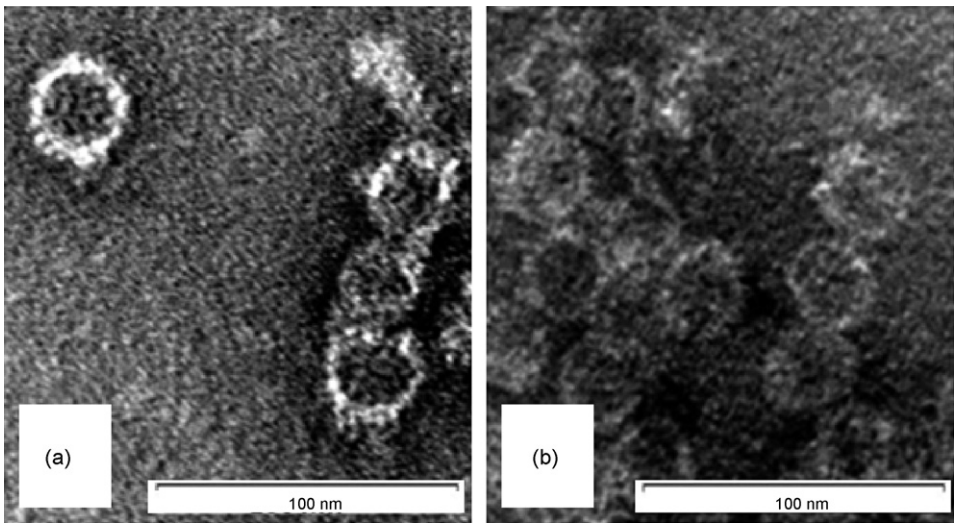

Fig. 7. Electron micrographs of the empty HBcAg particles and the HBcAg particles harbouring GFP. Electron micrographs showing the empty HBcAg particles (without any treatment) and HBcAg particles containing GFP. (a) Empty HBcAg. (b) HBcAg treated with 2.5 M urea and GFP was added before the association. Scale bar 100 nm.

demonstrates that the cargo remains associated with the particles for at least 1 month.

To confirm the capture of GFP by the 6-nm HBcAg subunits, the HBcAg particles were dissociated into the 6-nm species and fractionated on a sucrose gradient containing 2.5 M urea. These molecules were found to accumulate at the top of the gradient between fractions 20–24 (Fig. 5). Dialysis of these molecules in the presence of GFP resulted in the encapsidation of GFP in the HBcAg particles as proven by native agarose gel electrophoresis and TEM analysis (data not shown).

4. Discussion

HBcAg particles have been used widely as carriers to display foreign epitopes which are constructed by inserting their DNA coding sequences into the 5′-end, 3′-end or the centre of the HBcAg gene via recombinant DNA technique (Murray and Shiau, 1999; Pumpens and Grens, 2001). The cloning approach limits the flexibility of the cargo, confining it to be fused covalently and statically to HBcAg. In addition, only peptides or proteins encoded by nucleic acids can be fused to HBcAg through this approach. By employing this approach, Beterams et al. (2000) fused the 17-kDa *S. aureus* nuclease to the C-terminal end of HBcAg, displaying the nuclease in the interior of HBcAg particles. GFP and the outer surface lipoprotein (Osp) C of *Borrelia burgdorferi* had been linked covalently to the immunodominant region of HBcAg, displaying the proteins on the surface of the HBcAg particles (Kratz et al., 1999; Skamel et al., 2006; Vogel et al., 2005). Most recently, Nassal et al. (2008) displayed the entire 255-amino acid ectodomain of OspA and the dimeric OspC of *B. burgdorferi* on the surface of HBcAg particles through the internal insertion of HBcAg. Although this approach has been widely used to

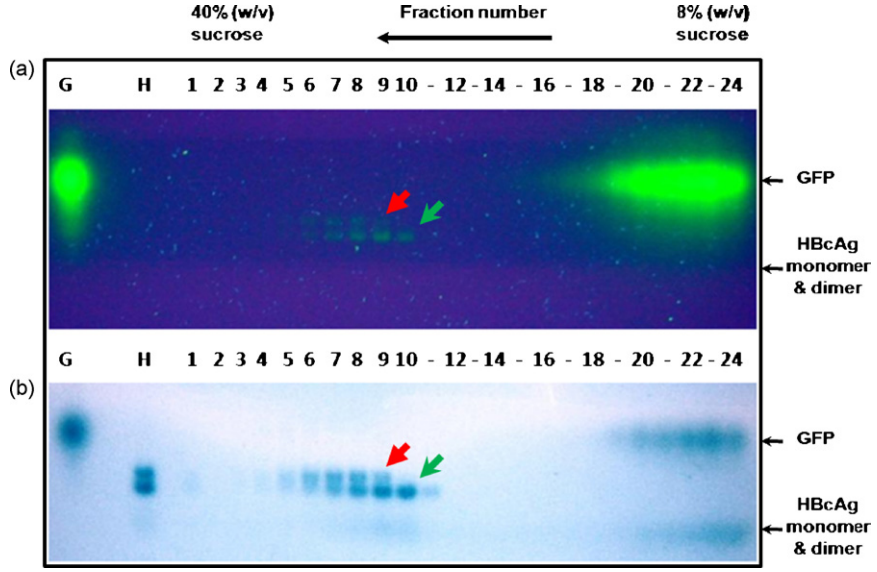

Fig. 8. Native agarose gel electrophoresis. Aliquots from the gradient fractions which corresponded to Fig. 6b were analysed on 1.5% (w/v) agarose gel and visualised by (a) UV illumination, and (b) Coomassie blue staining. Lanes G and H are GFP and HBcAg particles, respectively, which serve as controls. Two distinct bands in fractions 4–9 (red arrow) and fractions 5–11 (green arrow) show the migration profiles of the large and small HBcAg particles, respectively. (For interpretation of the references to colour in this figure legend, the reader is referred to the web version of the article.)

display immunogens for vaccine development, it limits the application of HBcAg particles as a free cargo container in drug delivery systems.

The present study has provided a better understanding of the association and dissociation of HBcAg particles by GdnHCl and urea. The HBcAg particles can be dissociated into two species of molecules: 6 nm and <1 nm. The former is believed to be the precursor for the association of the HBcAg particles of about 35 nm. The latter with a diameter of less than 1 nm is likely to be a totally denatured HBcAg which lost its assembly property. Here we showed that GdnHCl and urea exhibited an irreversible denaturation at concentrations more than 3 and 4 M, respectively. By referring to the model of the HBV capsid assembly proposed by Zlotnick et al. (1999), the dissociation of recombinant HBcAg particles by ≥3 M GdnHCl and ≥4 M urea is strongly believed to have blocked the pathway of trimeric nucleus formation of the HBcAg dimers, thus terminating the re-association route of HBcAg. However, we have proven in this study that 2.5 M of urea did not affect the assembly property of HBcAg and the fluorescent activity of GFP.

A number of denaturing agents have been employed to study the stability of viral capsids. Yang and Teng (1998) demonstrated an irreversible unfolding of the polyomavirus major capsid protein VP_1 by GdnHCl. Colomar et al. (1993) reported a technique of disrupting simian virus 40 (SM40) by using dithiothreitol (DTT) and EGTA to alter the disulfide bonds and calcium ion content of the viral particles. By employing the same method, human papillomavirus-like particles (Malboeuf et al., 2007; Touze and Coursaget, 1998) and recombinant rabbit hemorrhagic disease virus capsid (Mehdaoui et al., 2000) were disrupted. In this study, we showed that GdnHCl irreversibly denatured HBcAg particles. On the other hand, HBcAg tolerated the denaturing activity of urea at 2.5 M and it reassembled into core particles when the urea was removed.

Currently, limited information is available regarding the thermal stability of the particles formed by truncated HBcAg. In the current study, TEM analysis of the recombinant HBcAg particles following incubation at 70 °C for 1 h revealed intact particles with icosahedral symmetry. However, all the particles were structurally disrupted at 80 °C. This result is in agreement with the study conducted by Nath et al. (1992), whereby the immunoreactivity of the full-length HBcAg was retained when heated at 70 °C for 1 h but was inactivated at 85 °C in 10 min. Indirectly our study shows that the arginine-rich C-terminal end of HBcAg does not play an important role in the heat stability of the particles formed. The information about the thermal stability of the recombinant HBcAg particles may facilitate the design of a more protective delivery system.

A method to capture GFP was established by dissociating the HBcAg particles into the 6-nm molecule in the presence of urea and subsequently the denaturant was removed by dialysis. The GFP was found to be active and encapsidated inside the HBcAg particles for at least 1 month at 4 °C. Cargo accommodated by this method can be captured easily and released from the particles at a targeted destination. The HBcAg particles can be genetically engineered or chemically cross-linked to display a host-binding molecule such as an antibody or a ligand that facilitates the delivery of the cargo to target cells. For examples, bi-specific antibodies directed against receptors or cancer cell membranes were attached to the surface of bacterially derived 400 nm particles and used to deliver cytotoxic drugs to cancer cells (MacDiarmid et al., 2007). In the current study, GFP was used as a model for encapsidation, however the cargo is not limited to proteins, other molecules such as nucleic acids, analogues, antiviral agents and chemical compounds can also be packaged. The novelty of this new method implies further the broader exploitation of the HBV capsid as a carrier, making it a potential container for the development of a delivery system with high occupier flexibility.

Acknowledgements

The authors would like to thank Prof. Sir K. Murray for providing plasmid pR1-11E, and Dr. C.S. Tan for the plasmid pRSETGFP. The authors thank M.Y.T. Ng and S.T. Ong for technical supports. This work was supported by the FRGS Grant # 01-01-07-161FR and the Science Fund # 03-01-04SF0015.

References

Beterams, G., Böttcher, B., Nassal, M., 2000. Packaging of up to 240 subunits of a 17 kDa nuclease into the interior of recombinant hepatitis B virus capsids. FEBS Lett. 481, 169–176.

Böttcher, B., Tsuji, N., Takakashi, H., Dyson, M.R., Zhao, S., Crowther, R.A., Murray, K., 1998. Peptides that block hepatitis B virus assembly: analysis by cryomicroscopy, mutagenesis and transfection. EMBO J. 17, 6839–6845.

Bradford, M.M., 1976. A rapid and sensitive method for the quantitation of microgram quantities of protein utilizing the principle of protein–dye binding. Anal. Biochem. 72, 248–254.

Bringas, R., 1997. Folding and assembly of hepatitis B virus core protein: a new model proposal. J. Struct. Biol. 118, 189–196.

Burrell, C.J., MacKay, P., Greenaway, P.J., Hofschneider, P.-H., Murray, K., 1979. Expression in *Escherichia coli* of hepatitis B virus DNA sequences cloned in plasmid pBR322. Nature 279, 43–47.

Colomar, M.C., Degoumois-Sahli, C., Beard, P., 1993. Opening and refolding of simian virus 40 and in vitro packaging of foreign DNA. J. Virol. 67, 2779–2786.

Crowther, R.A., Kiselev, N.A., Böttcher, B., Berriman, J.A., Borisova, G.P., Ose, V., Pumpens, P., 1994. Three-dimensional structure of hepatitis B virus core particles determined by electron cryomicroscopy. Cell 77, 943–950.

Dane, D.S., Cameron, C.H., Briggs, M., 1970. Virus-like particles in serum of patients with Australia antigen-associated hepatitis. Lancet 295, 695–698.

Ganem, D., 1991. Assembly of hepadnaviral virions and subviral particles. Curr. Topics Microbiol. Immunol. 168, 61–83.

Jung, M.-C., Pape, G.R., 2002. Immunology of hepatitis B infection. Lancet Infect. Dis. 2, 43–50.

Kratz, P.A., Böttcher, B., Nassal, M., 1999. Native display of complete foreign protein domains on the surface of hepatitis B virus capsids. Proc. Natl. Acad. Sci. U.S.A. 96, 1915–1920.

Löffler-Mary, H., Dumortier, J., Klentsch-Zimmer, C., Prange, R., 2000. Hepatitis B virus assembly is sensitive to changes in the cytosolic S loop of the envelope proteins. Virology 270, 358–367.

MacDiarmid, J.A., Mugridge, N.B., Weiss, J.C., Phillips, L., Burn, A.L., Paulin, R.P., Haasdyk, J.E., Dickson, K.A., Brahmbhatt, V.N., Pattison, S.T., James, A.C., Al Bakri, G., Straw, R.C., Stillman, B., Graham, R.M., Brahmbhatt, H., 2007. Bacterially derived 400 nm particles for encapsulation and cancer cell targeting of chemotherapeutics. Cancer Cell 11, 431–445.

Malboeuf, C.M., Simon, D.A.L., Lee, Y.-E.E., Lankes, H.A., Dewhurst, S., Frelinger, J.G., Rose, R.C., 2007. Human papillomavirus-like particles mediate functional delivery of plasmid DNA to antigen presenting cells in vivo. Vaccine 25, 3270–3276.

Mehdaoui, S.E., Touze, A., Laurent, S., Sizaret, P.-Y., Rasschaert, D., Coursaget, P., 2000. Gene transfer using recombinant rabbit hemorrhagic disease virus capsids with genetically modified DNA encapsidation capacity by addition of packaging sequences from the L1 or L2 protein of human papillomavirus type 16. J. Virol. 74, 10332–10340.

Murray, K., Shiau, A.L., 1999. The core antigen of hepatitis B virus as a carrier for immunogenic peptides. Biol. Chem. 380, 277–283.

Nassal, M., Rieger, A., Steinau, O., 1992. Topological analysis of the hepatitis B virus core particle by cysteine–cysteine cross-linking. J. Mol. Biol. 225, 1013–1025.

Nassal, M., Skamel, C., Vogel, M., Kratz, P.A., Stehle, T., Wallich, R., Simon, M.M., 2008. Development of hepatitis B virus capsids into a whole-chain protein antigen display platform: new particulate Lyme disease vaccines. Int. J. Med. Microbiol. 298, 135–142.

Nath, N., Hickman, K., Nowlan, S., Shah, D., Phillips, J., Babler, S., 1992. Stability of the recombinant hepatitis B core antigen. J. Clin. Mirobiol. 30, 1617–1619.

Newman, M., Suk, F.-M., Cajimat, M., Chua, P.K., Shih, C., 2003. Stability and morphology comparisons of self-assembled virus-like particles from wild-type and mutant human hepatitis B virus capsid proteins. Virology 77, 12950–12960.

Pumpens, P., Grens, E., 2001. HBV core particles as a carrier for B cell/T cell epitopes. Intervirology 44, 98–114.

Roseman, A.M., Berriman, J.A., Wynne, S.A., Butler, P.J.G., Crowther, R.A., 2005. A structural model for maturation of the hepatitis B virus core. Proc. Natl. Acad. Sci. U.S.A. 102, 15821–15826.

Seitz, S., Urban, S., Antoni, C., Böttcher, B., 2007. Cryo-electron microscopy of hepatitis B virions reveals variability in envelope capsid interactions. EMBO J. 26, 4160–4167.

Skamel, C., Ploss, M., Böttcher, B., Stehle, T., Wallich, R., Simon, M.M., Nassal, M., 2006. Hepatitis B virus capsid-like particles can display the complete, dimeric outer surface protein C and stimulate production of protective antibody responses against *Borrelia burgdorferi* infection. J. Biol. Chem. 281, 17474–17481.

Tan, W.S., Dyson, M.R., Murray, K., 1999. Two distinct segments of the hepatitis B virus surface antigen contribute synergistically to its association with the viral core particles. J. Mol. Biol. 286, 797–808.

Tan, W.S., Dyson, M.R., Murray, K., 2003. Hepatitis B virus core antigen: enhancement of its production in *Escherichia coli*, and interaction of the core particles with the viral surface antigen. Biol. Chem. 384, 363–371.

Tan, W.S., McNae, L.W., Ho, K.L., Walkinshaw, M.D., 2007. Crystallization and X-ray analysis of the $T = 4$ particle of hepatitis B capsid protein with an N-terminal extension. Acta Crystallogr. Sect. F Struct. Biol. Cryst. Commun. F63, 642–647.

Touze, A., Coursaget, P., 1998. In vitro gene transfer using human papillomavirus-like particles. Nucleic Acids Res. 26, 1317–1323.

Vogel, M., Diez, M., Eisfeld, J., Nassal, M., 2005. In vitro assembly of mosaic hepatitis B virus capsid-like particles (CLPs): rescue into CLPs of assembly-deficient core protein fusions and FRET-suited CLPs. FEBS Lett. 579, 5211–5216.

Wingfield, P.T., Stahl, S.J., Williams, R.W., Steven, A.C., 1995. Hepatitis core antigen produced in *Escherichia coli*: subunit composition, conformational analysis, and in vitro capsid assembly. Biochemistry 34, 4919–4932.

Wynne, S.A., Crowther, R.A., Leslie, A.G., 1999. The crystal structure of the human hepatitis B virus capsid. Mol. Cell 3, 771–780.

Yang, Y.-W., Teng, C.-C., 1998. Stability of polyomavirus major capsid protein VP_1 under denaturants guanidine hydrochloride and urea. Int. J. Biol. Macromol. 22, 81–90.

Zheng, J., Schödel, F., Peterson, D.L., 1992. The structure of Hepadnaviral core antigens: identification of free thiols and determination of the disulfide bonding pattern. J. Biol. Chem. 267, 9422–9428.

Zlotnick, A., Johnson, J.M., Wingfield, P.W., Stahl, S.J., Endres, D., 1999. A theoretical model successfully identifies features of hepatitis B virus capsid assembly. Biochemistry 38, 14644–14652.